Sustainable Energy Technologies and Assessments 91 (2026) 105038

Contents lists available at ScienceDirect

Sustainable Energy Technologies and Assessments

journal homepage: www.elsevier.com/locate/seta

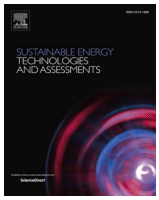

Original article

Enhancing thermal stability and oxidation resistance of engine lubricants by incorporating SiO_2 nanoparticles

Homeyra Piri [a], Vittoria Benedetti [b], Salar Moradi [a], Massimiliano Renzi [a,*], Marco Bietresato [a,c]

[a] Faculty of Engineering, Free University of Bozen-Bolzano I-39100 Bolzano, Italy
[b] Department of Civil, Environmental and Mechanical Engineering (DICAM), University of Trento I-38123 Trento, Italy
[c] Department of Agricultural, Food, Environmental and Animal Sciences (DI4A), University of Udine I-33100 Udine, Italy

ARTICLE INFO

Keywords:
Engine lubricants
Biolubricants
Nanoparticles
Oxidation
Thermal stability

ABSTRACT

Nanoparticles have emerged as promising additives for developing advanced engine lubricants capable of withstanding high temperatures and oxidative stress. This study investigates the potential of silicon dioxide (SiO_2) nanoparticles, surface-modified with KH570-Silane coupling agent, to enhance the oxidation resistance and thermal stability of lubricants and biolubricants. Thermal and oxidative properties were evaluated using thermogravimetric analysis (TGA), derivative thermogravimetry (DTG), and differential scanning calorimetry (DSC). The results revealed that increasing SiO_2 content has improved some critical thermal parameters, including onset, midpoint, inflection, and end temperatures. At 1.00 wt% SiO_2, the onset temperature of the biolubricant increased by 23.70 °C, reaching 345.30 ± 0.64 °C, while that of the lubricant increased by 24.55 °C, reaching 297.5 ± 1.84 °C. Maximum oxidation induction times of 29.65 ± 3.18 min (biolubricants) and 27.70 ± 1.04 min (lubricants), along with enthalpy values of 509.45 ± 26.8 $J{\cdot}g^{-1}$ and 459.85 ± 12.66 $J{\cdot}g^{-1}$, respectively, were achieved at the same concentration. These findings demonstrate that surface-modified SiO_2 nanoparticles significantly enhance the thermal stability and oxidation resistance of both conventional and bio-based lubricants, highlighting nanoparticles' potential to improve engine performance, extend possible industrial applications, and theoretically extend oil-change intervals, with obvious environmental and economic benefits.

Introduction

Engine lubricants are essential for machinery maintenance and operation [1–4]. Lubricants are employed in any area of a vehicle where metal components are in relative motion to one another. Their primary responsibilities are to lessen surface friction, dissipate heat, and stop part rusting and corrosion [5,6]. However, considering the harsh conditions of operation that engines face, such as high temperatures and oxidative environments, lubricants with enhanced thermal stability and oxidation resistance are needed [7–9].

Despite their widespread use and well-established performance, commonly employed multigrade engine lubricants such as SAE 10W40 and SAE 15W40 still exhibit intrinsic limitations under prolonged high-temperature and oxidative operating conditions [10]. Experimental studies and field reports have shown that these formulations are prone to oxidative thickening, depletion of antioxidant packages, and deposit formation when exposed to sustained thermal stress, particularly in modern engines operating under higher loads and extended drain intervals [11–14]. These degradation mechanisms ultimately limit lubricant lifetime and motivate the search for improved stabilization strategies.

Although conventional additive packages enhance lubricant performance, they have drawbacks as well. Indeed, detergents and anti-wear additives can encourage the production of deposits on parts subjected to high temperatures [15,16]. Dispersants and detergents can make anti-foam compounds less effective, which can result in foaming [17–19], and high temperatures can cause some additives to corrode metals [16,17]. Viscosity index enhancers with a high molecular weight, subjected to permanent mechanical shear in gears, can manifest significant viscosity loss and this fact can lead to a poor lubrication of mechanical components [17]. High-temperature applications can cause the formation of ash deposits originated from metal-based detergent additives,

* Corresponding author.
E-mail addresses: homeira.piri@gmail.com (H. Piri), vittoria.benedetti@unitn.it (V. Benedetti), salar.moradi@unibz.it (S. Moradi), massimiliano.renzi@unibz.it (M. Renzi), marco.bietresato@uniud.it (M. Bietresato).

https://doi.org/10.1016/j.seta.2026.105038
Received 14 September 2025; Received in revised form 27 March 2026; Accepted 14 May 2026

[17], and extreme pressure agents that use Sulphur and Phosphorus compounds can attack yellow metals and become corrosive [17,20]. Long-term deterioration or depletion of these compounds may lessen their efficacy, requiring more frequent oil changes and, thus, posing environmental issues. Consequently, while conventional additive packages are effective in the short term, their thermal instability, potential corrosivity, and progressive depletion under severe operating conditions represent fundamental constraints for long-term lubricant performance.

In view of the drawbacks of conventional additives, adding nanoparticles/nanosystems to lubricants (to have the so-called "nanolubricants") is thought to be one of the best ways to enhance lubricants' tribological properties, increase their thermal stability, prevent oxidation and lower friction and wear-and-tear phenomena in the metal surfaces. Such advancements have a significant direct and indirect positive influence on the environment: (1) the prolongation of the durability over time can extend oil-change intervals (net of possible cross-contaminations between lubricant and fuel [21]), (2) the prevention of a significant decay of properties helps keeping high the engines' overall efficiency, thus reducing greenhouse gas emissions and energy consumption [4].

In order to study the influence of nanoparticles and nanosystems on the thermal stability and oxidation resistance of lubricants and biolubricants, techniques such as thermogravimetric analysis (TGA) coupled with derivative thermogravimetry (DTG), and differential scanning calorimetry (DSC) are usually adopted. In particular, TGA provides essential insights into a material's composition, thermal stability, and decomposition kinetics by monitoring mass changes under controlled temperature programs [22,23]. Conversely, DSC measures heat flows associated with temperature-induced transitions, enabling the detection of possible endothermic and exothermic events occurring during exposures to thermal changes, and the quantification of the corresponding enthalpy variations [24–27].

For instance, Abdul Khaliq et al. [28] employed TGA to examine the thermal degradation of mineral lubricants modified with graphene. Graphene flakes with thicknesses of 8 nm, 12 nm, and 60 nm as well as engine lubricants 20W50 SN/CF and 20W50 SJ/CF were utilized to prepare a variety of samples. TGA showed that the inclusion of graphene could improve the thermal stability of SN/CF lubricants delaying their oxidation onset temperature by 13–17 °C. Furthermore, when the sample experienced between 20% and 40% weight loss, the oxidation onset temperature could be increased by more than 30 °C. The size and concentration of graphene flakes have a significant impact on the lubricant resistance to degradation. According to TGA kinetics studies, indeed, the use of graphene considerably lowers the activation energy (Ea), which is larger in base oils. This indicates a change in the kinetics of decomposition and suggests that the resulting nanolubricant is more thermally stable under oxidative conditions than the starting lubricant.

Maheswaran et al. [29] investigated the impact of dispersing 0.25 wt %, 0.50 wt%, and 0.75 wt% of nano garnet particles in SN500-grade gear lubricant. DSC and TGA methods demonstrated that adding 0.75 wt% nano-garnet particles to this lubricant significantly raises the decomposition temperature, shifting it from 255 °C to 425 °C, and conferring the nanolubricant under study the ability to withstand mass loss when heated from 175 °C to 240 °C compared to the lubricant without nano garnet particles.

Ramachandran et al. [30] investigated how the dispersion of NiO nanoparticles into SN500 lubricant affected its non-isothermal heat stability. TGA, DSC, and Differential Thermal Analysis (DTA) are used to determine thermal stability. Low concentrations of nanoparticles (up to 0.3 wt%) in NiO-nanolubricants resulted in the maximum obtainable thermal stability. At 200 °C, the SN500 lubricant loses 9.5% of its mass, while the associated nanolubricant with NiO-nanoparticles having a concentration of 0.1 wt% and 0.3 wt% do not lose any mass, thus proving that NiO-nanolubricant can be utilized for temperature-dependent applications.

Mohamed Kamal et al. [31] used a simultaneous thermal analyzer (TGA/DTG/DSC) to investigate lubricants' thermal degradation. In comparison to the reference oil (5W30), the results demonstrated that Al_2O_3/TiO_2 hybrid nanolubricants could postpone the oxidation onset temperature and the burnout temperature by 54.9 °C and 38.7 °C, respectively.

Ibrahim Ogu Sadiq [32] demonstrated that biolubricants (obtained from coconut oil, in this case) containing graphene or maghemite nanoparticles at 0.1 vol% (≈0.24 wt% graphene; ≈0.56 wt% maghemite) were resistant to oxidation. The oxidation onset temperature of the nano-charged biolubricants was raised by 18.75 °C for maghemite-charged nanolubricant (MGCO), and by 37.5 °C for graphene-charged nanolubricant (XGCO). This enhancement has a positive impact on tribological performance and viscosity. Wear scar diameter (WSD) and coefficient of friction (COF) decreased by 10.40% and 5.60%, respectively, for XGCO, and by 3.43% and 4.30%, for MGCO in comparison to coconut oil. Finally, the viscosity index of graphene and maghemite nanolubricants was increased by 13.85% and 7.36%, respectively.

Although numerous studies have investigated nanoparticle-enhanced lubricants, most available works focus predominantly on tribological performance [33–35], with limited attention to systematic thermal and oxidative stability metrics derived from integrated TGA, DTG, and DSC analyses. Moreover, direct comparisons between mineral-based and commercially available bio-based engine lubricants under identical experimental conditions remain scarce. In particular, the combined effects of surface-modified SiO_2 nanoparticles on oxidation onset, degradation kinetics, and oxidation induction time have not been comprehensively quantified. This lack of integrated thermal–oxidative assessment represents a clear research gap that the present study aims to address [36]. Despite the fact that SiO_2 is intrinsically an electrically insulating material with low intrinsic thermal conductivity [37–39], its contribution to oxidation resistance is not associated with electronic charge transport, in contrast to graphene-based additives, whose performance can involve conductive or percolative heat-transfer pathways [40,41]. Instead, well-dispersed SiO_2 nanoparticles act as physical barriers that hinder oxygen diffusion and radical propagation within the lubricant matrix. Additionally, the KH570 silane shell enhances interfacial compatibility, promoting homogeneous dispersion and reducing localized thermal hotspots [42]. Unlike graphene, whose performance is often linked to percolation effects and high aspect ratio, SiO_2 provides stabilization through interfacial and barrier mechanisms, offering a complementary and potentially more formulation-robust approach to oxidation inhibition [43,44].

It was shown in another previous investigation by the authors [42], that adding SiO_2 nanoparticles coated with the silane coupling agent KH570 greatly improves the physicochemical characteristics of both conventional lubricants (Mistral 15W40) and biolubricants (PLANTO MOT SAE 10W40). Surface modification allowed for a better dispersion of SiO_2 nanoparticles and, thus, a more stable suspension of nanoparticles in the lubricant volume. The results showed slight increases in density and viscosity, along with a higher viscosity index. Total Base Number (TBN) and Total Acid Number (TAN) analysis also verified that a strong alkaline reserve was maintained and that the addition of SiO_2 nanoparticles did not result in the introduction of critical acidity levels. The inductively coupled plasma optical emission spectroscopy (ICP-OES) also revealed that the addition of SiO_2 nanoparticles primarily influences the concentration of Silicon, with slight effect on other additives. Without changing the fundamental functional structures of the lubricants and biolubricants, a Fourier Transform Infrared (FTIR) analysis verified the presence of SiO_2 and KH570, demonstrating exceptional chemical stability. However, that investigation primarily focused on the physicochemical properties and chemical stability of the nanolubricants, without addressing their thermal stability, oxidative resistance, or their temperature-dependent evolution, which are critical for evaluating real-world lubricant performance.

Most published studies on SiO_2 nanoparticle additives concentrate on their effects on the tribological properties of the resulting

nanolubricant (in particular, the obtainable reductions in friction and wear-and-tear phenomena) but rarely examine the induced modifications on the chemical or oxidative stability [45,46]. In this context, the present work represents the first integrated TGA/DTG/DSC evaluation of KH570-modified SiO_2 nanoparticles in both a mineral-based and a bio-based SAE 40 lubricant, including polynomial trend modelling of key thermal and oxidative stability metrics. By combining thermogravimetric, calorimetric, spectroscopic, and chemical analyses (TGA, DTG, DSC, FTIR, ICP-OES, and TBN/TAN), and by directly comparing mineral and biolubricant formulations under identical conditions, this study provides a comprehensive and quantitative framework that extends beyond conventional tribology-focused investigations. In contrast, by performing these tests on both a biolubricant and a mineral-based lubricant, this study offers comparative insights that are absent from earlier tribology-only studies.

Continuing the study of the properties of these two lubricants, as representative of their respective classes of lubricants (i.e., conventional and bio-based, respectively), this study investigates the potential advantages, in terms of thermal stability and oxidation resistance, obtainable thanks to the use of SiO_2 nanoparticles coated with KH570-Silane coupling agent. SiO_2 nanoparticles are widely reported as chemically inert materials whose biological and environmental impacts strongly depend on particle size, concentration, and exposure pathway, rather than representing intrinsic non-toxicity or universal biocompatibility. In lubricant applications, where nanoparticles are fully dispersed and embedded within an oil matrix, direct biological exposure is minimized, allowing their functional advantages to be exploited without implying inherent safety or environmental benignity [47,48]. Importantly, their ability to significantly reduce friction and wear-and-tear phenomena between components in relative motion makes them particularly promising as lubricant additives. As declared above, the used biolubricant and conventional lubricant are the same of the previous study: the PLANTO MOT SAE 10W40, and the Mistral 15W40. The chosen biolubricant (PLANTO MOT SAE 10W40) was selected as an example of cutting-edge biodegradable engine oils due to its unique properties and wide range of applications. Since Mistral 15W40 is, instead, a mineral-based lubricant that is considered industry standard, it was chosen as well as a benchmark for performance comparison. These two lubricants have the same SAE 40 high-temperature viscosity rating. By pairing them, we maintain comparable high-temperature viscosity while representing distinct lubricant categories. From a sustainability perspective, this performance-based comparison allows the benefits of KH570-modified SiO_2 additives to be generalized across real-world lubricant formulations through enhanced durability, reduced friction, and extended lubricant service life, rather than relying on claims of intrinsic environmental friendliness [36,49]. Thanks to these evidences, the results of the investigation are applicable to industrial machinery and automobile applications.

A comprehensive investigation was conducted utilizing TGA, DTG, and DSC to determine the impact of SiO_2 nanoparticles on the thermal and oxidative characteristics of the lubricants.

Materials and methods

Materials

Lubricants utilized in this investigation were PLANTO MOT SAE 10W40, a biolubricant produced by FUCHS LUBRICANTS GERMANY GmbH (Mannheim, Germany, https://www.fuchs.com/de/en/), and Mistral 15W40, a conventional lubricant by NILS S.p.A. (Postal, Bolzano, Italy; https://www.nils.eu/en/). Tables 1 provides a full description of the technical specifications of these two lubricants. The nanoparticles were provided by Nanografi Inc. (Çankaya/Ankara, Turkey; https://nanografi.com/). Their details are reported in Tables 2 and 3.

Table 1
Technical characteristics of the two lubricants considered in this study.

Property	Measurement Unit	Reference	NILS Mistral 15W40	PLANTO MOT SAE 10W40
Density at 15 °C	[g·cm^{-3}]	ASTM D4052–22 [50]	0.8769	0.8719
Kinematic viscosity at 40 °C	[mm^2·s^{-1}]	ASTM D445-24 [51]	97.3	87.0
Kinematic viscosity at 100 °C	[mm^2·s^{-1}]	ASTM D445-24 [51]	13.5	13.7
Viscosity index	[−]	ISO 2909:2002 [52]	138	160
TBN	[mg(KOH)·g^{-1}]	ASTM D4739-17 [53]	10.5	9.7
TAN	[mg(KOH)·g^{-1}]	ASTM D664-18e2 [54]	2.2	1.7

Table 2
Silicon dioxide (SiO_2) nanoparticles coated with KH570-Silane coupling agent properties.

Technical Property	Measurement Unit	Value / Appearance
Purity	[%]	95.9
Colour	[−]	white
Average Particle Size	[nm]	18–35
Specific Surface Area	[m^2·g^{-1}]	150–550
Bulk Density	[g·cm^{-3}]	<0.1
True Density	[g·cm^{-3}]	2.2

Table 3
Elemental Analysis of SiO_2 nanoparticles coated with KH570-Silane coupling agent.

Element	wt%
SiO_2	95.9
KH570	3–4
Fe	0.032
Ca	0.056
Mg	0.0085
S	0.025

Preparation of nanolubricants samples

Nanoparticles were distributed in PLANTO MOT SAE 10 W-40 biolubricant and Mistral 15W40 lubricant at four different mass percent concentrations (i.e.: 0.25, 0.50, 0.75, and 1.00 wt%). The literature's recommendations for the most effective ranges of SiO_2 nanoparticles in lubricants were used to choose these concentrations [55,56]. Following the addition of the nanoparticles, the samples were magnetically stirred for 1.5 h at ambient temperature at 1500 rpm. After that, an ultrasonic cleaner (model USC 600 THD by VWR, Radnor, Pennsylvania, USA; https://www.vwr.com/) with a 120-W-power output and a 45-kHz-frequency was used for 2.5 h. During ultrasonication, the bath temperature was monitored and remained below 35 ± 5 °C, ensuring that no unintended thermal aging of the lubricant occurred. Stability and dispersion of the samples were assessed in a prior work of the authors using sedimentation photography, FTIR spectroscopy, and UV–Vis spectrophotometric analyses [42]. A summary of the physicochemical characteristics of the obtained nanolubricants and nanobiolubricants is given in Table 4 and Table 5. For these tables, properties are reported as representative values reproduced from Ref.[42], in which replicate-based standard deviations were not reported; instrument calibration and measurement accuracy follow manufacturer specifications.

Table 4
Physicochemical properties of the tested nanolubricants [42].

Property	Lubricant (pure) Mistral 15W40	Nanolubricant 0.25% SiO_2	Nanolubricant 0.50% SiO_2	Nanolubricant 0.75% SiO_2	Nanolubricant 1.00% SiO_2
Appearance	dark yellow	dark yellow	dark yellow	dark yellow	dark yellow
Smell	characteristic	characteristic	characteristic	characteristic	characteristic
Density at 15 °C [g·cm^{-3}]	0.8769	0.8808	0.8819	0.8831	0.8842
Viscosity at 40 °C [mm^2·s^{-1}]	97.3	97.6	98.4	99.0	99.9
Viscosity at 100 °C [mm^2·s^{-1}]	13.5	13.7	13.8	13.9	14.0
Viscosity Index [-]	138	141	142	142	143
TAN [mg(KOH)·g^{-1}]	2.17	1.9	1.9	2.1	2.2
TBN [mg(KOH)·g^{-1}]	10.6	10.7	10.3	10.3	10.3
POLLUTION [ppm]					
Silicon	65	419	738	1101	1365
Sodium	0	0	0	0	2
ADDITIVES [ppm]					
Calcium	3045	3118	3124	3084	3043
Magnesium	71	71	72	74	70
Zinc	928	926	923	915	889
Phosphorus	766	827	798	809	795
Boron	137	131	131	130	126
Molybdenum	6	9	9	9	9

Table 5
Physicochemical properties of the tested nanobiolubricants [42].

Property	Biolubricant (pure) SAE 10W40	Nanobiolubricant 0.25% SiO_2	Nanobiolubricant 0.50% SiO_2	Nanobiolubricant 0.75% SiO_2	Nanobiolubricant 1.00% SiO_2
Appearance	dark yellow	dark yellow	dark yellow	dark yellow	dark yellow
Smell	characteristic	characteristic	characteristic	characteristic	characteristic
Density at 15 °C [g·cm^{-3}]	0.8719	0.8733	0.8746	0.8758	0.877
Viscosity at 40 °C [mm^2·s^{-1}]	87.0	87.9	88.6	89.6	90.3
Viscosity at 100 °C [mm^2·s^{-1}]	13.7	14.0	14.2	14.3	14.4
Viscosity Index [-]	160	164	165	166	166
TAN [mg KOH·g^{-1}]	1.7	2.2	2.4	2.5	2.6
TBN [mg KOH·g^{-1}]	9.7	9.5	9.6	9.9	9.6
POLLUTION [ppm]					
Silicon	2	337	702	1020	1402
Sodium	0	0	0	0	5
ADDITIVES [ppm]					
Calcium	1672	1720	1737	1720	1761
Magnesium	333	345	353	351	359
Zinc	693	690	678	668	658
Phosphorus	593	596	594	587	591
Boron	487	472	459	462	476
Molybdenum	74	73	75	73	74

Analysis of thermal and oxidation characteristics

Thermogravimetric analysis (TGA) and derivative thermogravimetry analysis (DTG)

In this study, TGA was performed via a STA 449 F3 Jupiter thermogravimetric analyzer (Netzsch-Gerätebau GmbH, Selb, Germany; https://www.netzsch.com/) with a heating rate of 5.5 K·min^{-1} and temperatures ranging from 40 °C to 500 °C. Approximately 10 ± 0.1 mg of lubricant or biolubricant per sample was weighed and dropped in an alumina crucible for each test. Nitrogen was used both as purge and protective gas, with a flow rate of 20 mL·min^{-1} in both cases.

Each test was duplicated to ensure repeatability, following the procedure described by Benedetti et al. [57] and Pecchi et al. [58]. In most cases, key thermal parameters, such as onset temperature, maximum degradation temperature, and residual mass, differed by less than 2% between the replicates. As a general rule, if a deviation beyond this threshold had been observed, both measurements were discarded and the experiment was repeated until two valid replicates were obtained within the 2% acceptance threshold. Final (valid) values are reported in this document in terms of mean ± standard deviation calculated from duplicate measurements, acknowledging that the reported standard deviation reflects measurement repeatability rather than a population-based statistical uncertainty. A pooled standard deviation was not applied, as only two valid replicates were available for each experimental condition, which would not provide a statistically meaningful pooled estimate.

From the TGA and DTG analyses, key thermal transition points, namely the onset, midpoint, inflection, and end temperatures, were identified. The *onset temperature*, referred to as the initial oxidation or decomposition temperature, was determined by extrapolating the tangent to the initial mass-loss region on the TGA curve [59]. The *midpoint temperature* corresponds to the point at which 50% of the total mass-loss has occurred. The *inflection temperature* is defined as the temperature correspondent to the peak of the DTG curve, representing the maximum rate of mass-loss. Finally, the *end temperature* marks the point where the TGA curve levels off, indicating the completion of the primary decomposition process. To avoid ambiguity in the identification of thermal transition points across different instruments and software, a schematic representation of the construction method used in this study is provided below in Fig. 1.

Differential scanning calorimetry (DSC)

A DSC 200 F3 Maia differential scanning calorimeter (Netzsch-Gerätebau GmbH, Selb, Germany; https://www.netzsch.com/) was used to perform DSC at a heating rate of 5.5 K·min^{-1} at temperatures ranging from 40 °C to 500 °C, and the associated enthalpy (J·g^{-1}) was quantified

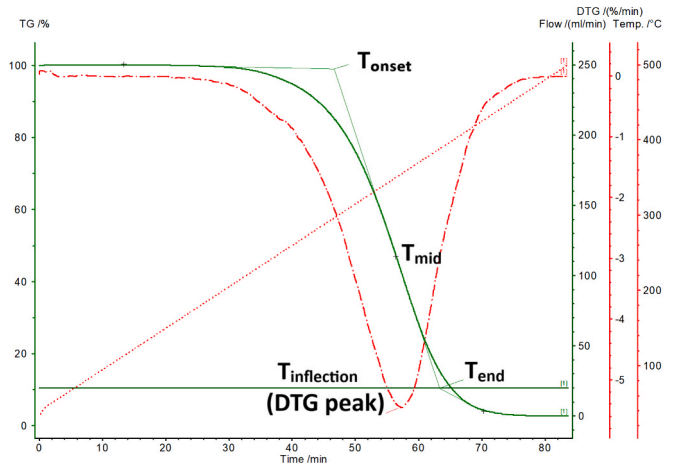

Fig. 1. Representative TG and DTG curves illustrating the definition of characteristic thermal transition points used in this study: onset temperature (T_{onset}), midpoint temperature (T_{mid}, 50% mass loss), inflection temperature ($T_{inflection}$, DTG peak), and end temperature (T_{end}). Moreover, the residual mass at 500 °C, an indicator of the char or ash content remaining after thermal degradation, was also measured to assess both the material's thermal stability and inorganic residue content [28,29].

by calculating the area under the exothermic peak in a Cartesian representation of the heating process (horizontal axis: time in minutes; vertical axis: heat flow in $mW \cdot mg^{-1}$), using Netzsch software.

The time interval between the start of oxygen exposure and the start of an exothermic oxidation reaction, as measured by DSC, is known as the Oxidation Induction Time (OIT), which is a crucial sign of the oxidative stability of a lubricant [60]. In this work, OIT was determined from dynamic DSC scans and defined as the time coordinate corresponding to the onset of the main exothermic oxidation peak, as identified using the onset criterion implemented in NETZSCH Proteus software.

Approximately 10 ± 0.1 mg of each lubricant or biolubricant per sample was weighed and sealed in an alumina crucible for each test. The crucible lid was pierced with a pin-hole to allow controlled gas exchange during OIT measurements. Nitrogen was used as purge gas to maintain an inert atmosphere, and its flow rate was set to 100 $mL \cdot min^{-1}$.

Each DSC test was repeated at least twice to ensure repeatability. In most cases, variation in onset temperature, peak position, and enthalpy values across replicates remained below 3%. When discrepancies exceeded this threshold, the test was repeated and the outlier excluded. Final results are reported in terms of mean ± standard deviation of the accepted replicates, with the understanding that the standard deviation reflects limited replicates and serves as an estimate of repeatability.

Results and Discussion

Thermal stability analysis

The thermal stability and the decomposition properties of the pure lubricant, the pure biolubricant, and all the presented blends of these two lubricants added with nanoparticles were investigated via TGA and DTG. The TGA plots of the pure lubricant and biolubricant, together with the corresponding nanolubricants and nanobiolubricants obtained with different SiO_2 wt% (0.25 wt%, 0.50 wt%, 0.75 wt%, and 1.00 wt%), are displayed in Fig. 2. In these plots, the vertical axis expresses the residual mass of the sample as a percentage of its initial mass (TG %). This normalized representation is common in thermogravimetric analysis (TGA) to allow easy comparison between samples regardless of the initial sample mass. The horizontal axis represents the elapsed time (in minutes), which corresponds to the progression of the heating program from the room temperature to 500 °C at a constant heating rate. Therefore, the mass loss trends observed over time reflect the thermal degradation profile of each sample.

Fig. 3 presents the comparative thermogravimetric analysis and derivative parameters of lubricants and biolubricants charged with SiO_2 nanoparticles, along with fitted quadratic curves, useful to individuate trends and maximum effects of nanoparticles on lubricants in correspondence to increasing concentrations of theirs.

The results of TGA and DTG analyses are summarized in Table 6 and Table 7, in which the values obtained for onset, midpoint, inflection, and end temperatures are reported. The tables present a summary of the TGA and DTG analyses for the lubricants and nanolubricants, including average values and standard deviations from replicate tests.

Biolubricants result more thermally stable than conventional lubricants, and their thermal stability increases with SiO_2 addition. Indeed, pure biolubricant shows higher average onset (321.6 ± 6.24 °C) and inflection temperatures (374.3 ± 4.31 °C), with the average onset temperature increasing by 23.7 °C at 1.00 wt% SiO_2, reaching 345.3 ± 0.64 °C, and the average inflection temperature increasing by 16.4 °C at 1.00 wt% SiO_2, thus reaching 390.7 ± 1.70 °C. Lower temperatures were observed in conventional lubricants, with average onset and average inflection temperatures of 272.95 ± 0.64 °C and 327.1 ± 6.51 °C, respectively. Although temperatures increased with the addition of nanoparticles, reaching an average onset of 297.50 ± 1.84 °C and an inflection temperature of 352.65 ± 3.61 °C at 1.00 wt% SiO_2 (absolute increases of 24.55 °C and 25.55 °C, respectively), values were still not comparable with those obtained for biolubricants (differences of about 47.8 °C in onset and 38.05 °C in inflection temperatures, in favor of biolubricants). The observed differences are more likely related to the different base oil composition and additive formulation of the two lubricants, rather than solely to their SAE grades. This behavior can be attributed to the ester-based structure of biolubricants, which typically exhibit higher polarity and a greater degree of molecular saturation compared to conventional mineral oils. These features promote stronger intermolecular interactions and improved resistance to thermo-oxidative chain scission, resulting in delayed degradation and higher inflection temperatures.

Polynomial fitting of these temperature-related parameters revealed a good correlation with SiO_2 content ($R^2 > 0.98$), confirming that quadratic equations can describe the trend effectively. It should be noted that the high R^2 values arise from the smooth, monotonic response of thermogravimetric parameters to SiO_2 concentration and from the limited number of experimental points (five levels), for which a second-order polynomial provides an appropriate empirical description of the observed trend rather than a predictive statistical model. Confidence intervals were not calculated due to the limited number of replicates (n = 2); therefore, standard deviation bands are reported to illustrate experimental dispersion. The fitted equations for onset temperature were:

$$y = -49.34 \cdot x^2 + 73.89 \cdot x + 272.95 \text{ (lubricant)} \quad (1)$$

$$y = -22.59 \cdot x^2 + 46.29 \cdot x + 321.60 \text{ (biolubricant)} \quad (2)$$

Looking at the Cartesian position of the vertex of these two parabolas, the optimal SiO_2 content for maximizing onset temperature was estimated at ~ 0.75 wt% for lubricant and ~ 1.00 wt% for biolubricant (NB: in this case, the upper mass-percentage limit was indicated, as the vertex is placed outside the inquired interval).

As the percentage of SiO_2 increases, the mass change for conventional lubricant falls from −83.81 ± 0.83% to −79.55 ± 0.4% (at 1.00 wt% SiO_2) as temperature increase, hence with a difference of 4.26 percentage points, suggesting lower thermal degradation. Polynomial fitting showed a good correlation with SiO_2 content ($R^2 > 0.98$), with the fitted equation for lubricant being:

$$y = -6.63 \cdot x^2 + 10.89 \cdot x + 83.81 \quad (3)$$

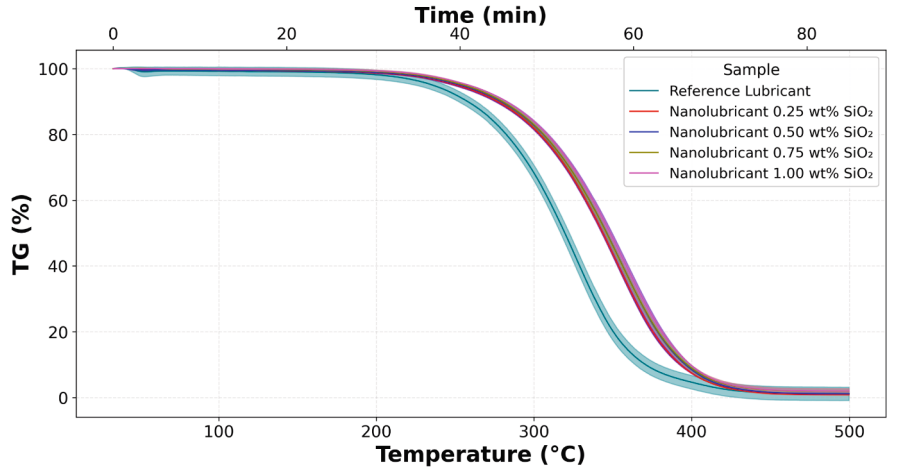

(a)

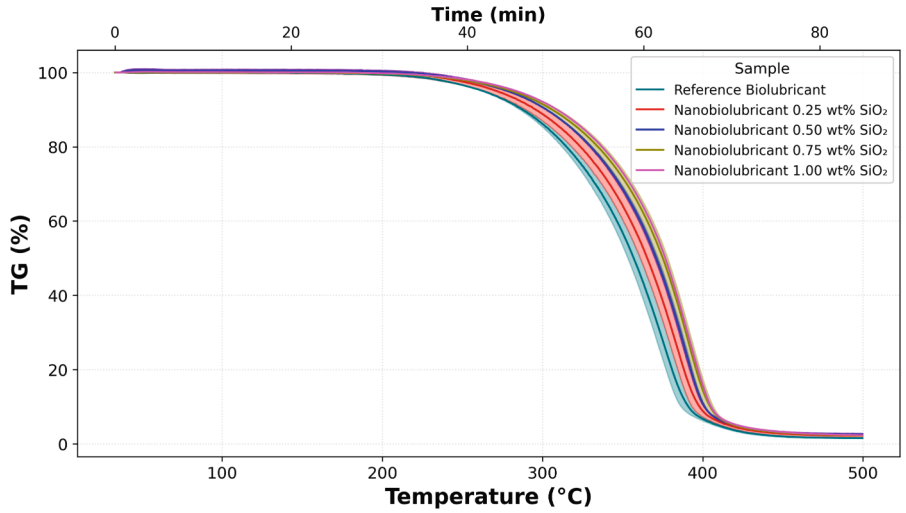

(b)

Fig. 2. TGA plots of nanolubricants (a) and nanobiolubricants (b) obtained under nitrogen atmosphere (N_2) at a heating rate of 5.5 K·min^{-1}. In both the plots, the central curves represent the average trends, and the surrounding shaded areas the dispersion of experimental values calculated as mean ± standard deviation (n = 2).

The optimal SiO_2 content for minimizing mass loss was estimated to be ~ 0.82 wt%.

However, for biolubricants, it rises from −86.42 ± 0.01% (pure) to −87.11 ± 0.01% (at 0.50 wt% SiO_2), and then drops to −86.88 ± 1.05% at 1.00 wt% SiO_2. Student's *t*-test analysis indicated that the differences in mass change between conventional and biolubricants were statistically significant ($p < 0.05$) at all SiO_2 concentrations, suggesting a consistent influence of base oil composition and additives on thermal stability. The corresponding polynomial fit for biolubricants was:

$$y = 1.42{\cdot}x^2 - 1.88{\cdot}x - 86.42 \quad (4)$$

With the minimum mass change occurring at ~ 0.66 wt% SiO_2.

Following thermal degradation, residual mass rises from 0.00% (pure) to 1.96 ± 1.04% (at 1.00 wt% SiO_2) for lubricants, and from 1.56 ± 0.07% (pure) to 2.37 ± 0.22% (at 1.00 wt% SiO_2) for biolubricants. This suggests the presence of thermally stable SiO_2 particles. The polynomial fitting indicated a strong correlation for both cases ($R^2 > 0.98$). The fitted equation for lubricant was:

$$y = -1.45{\cdot}x^2 + 3.41{\cdot}x \quad (5)$$

With an optimal SiO_2 content of ~ 1.18 wt%, while for biolubricant the fitted equation was:

$$y = -1.99{\cdot}x^2 + 2.80{\cdot}x + 1.56 \quad (6)$$

And the optimum was reached at ~ 0.70 wt%.

Slower degradation is shown by the maximum percentage mass loss rate, whose value was observed to decrease from −5.94 ± 0.05 %·min^{-1} (pure lubricants) to −5.42 ± 0.04 %·min^{-1} (at 1.00 wt% SiO_2) at temperatures from 327.55 ± 3.18 °C to 356.65 ± 2.47 °C as SiO_2 content is increasing. In contrast, the maximum mass loss rate for biolubricants is different and rises with increasing SiO_2 concentration from −7.62 ± 0.19 %·min^{-1} to −8.60 ± 0.07%·min^{-1}, at temperatures from 376.5 ± 6.22 °C to 393.9 ± 2.12 °C, suggesting a delayed, but more severe, thermal degradation. The fitted curves indicate the rate of mass loss reaches a minimum at 0.75 wt% and 0.75 wt% respectively:

$$y = -0.73{\cdot}x^2 + 1.25{\cdot}x + 5.94 \text{ (lubricant)} \quad (7)$$

$$y = +1.56{\cdot}x^2 - 2.54{\cdot}x - 7.62 \text{ (biolubricant)} \quad (8)$$

Meanwhile, the temperature at maximum degradation rate (T_{max}) increases polynomially with SiO_2 addition:

$$y = -55.06{\cdot}x^2 + 84.16{\cdot}x + 327.55 \text{ (lubricant)} \quad (9)$$

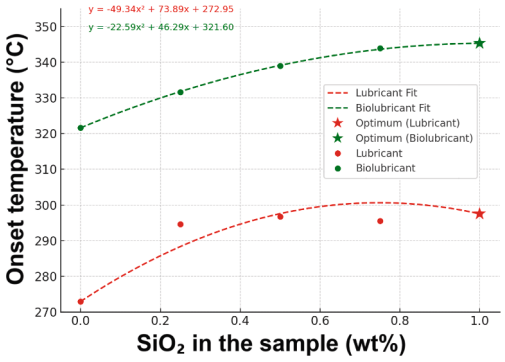

(a)

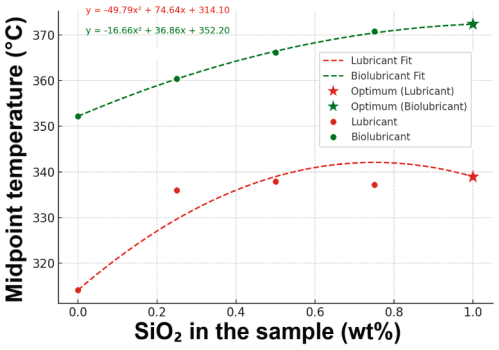

(b)

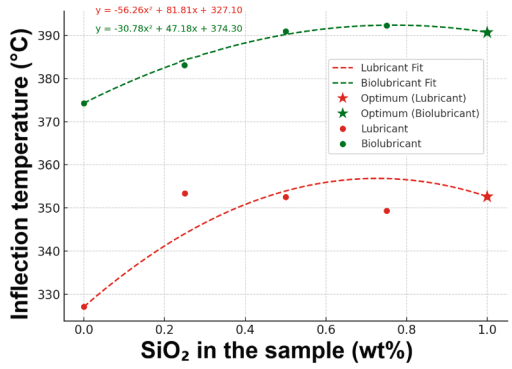

(c)

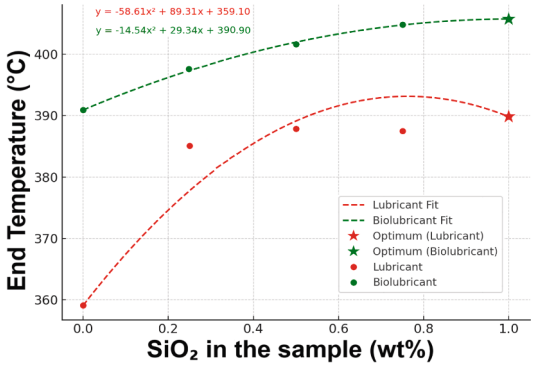

(d)

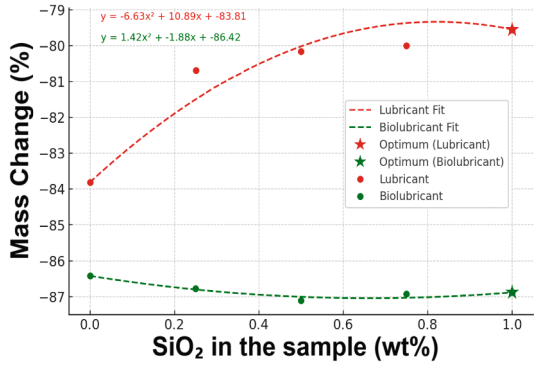

(e)

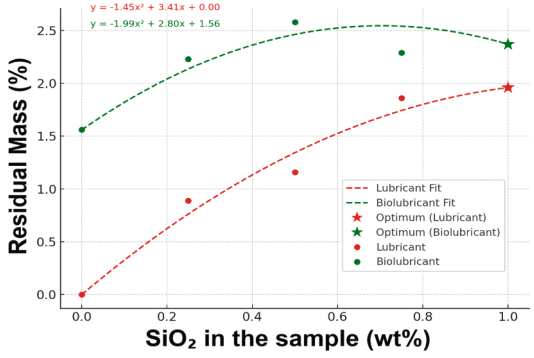

(f)

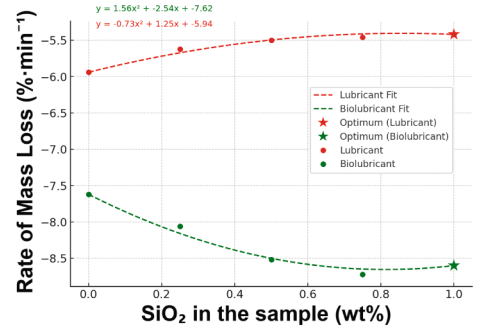

(g)

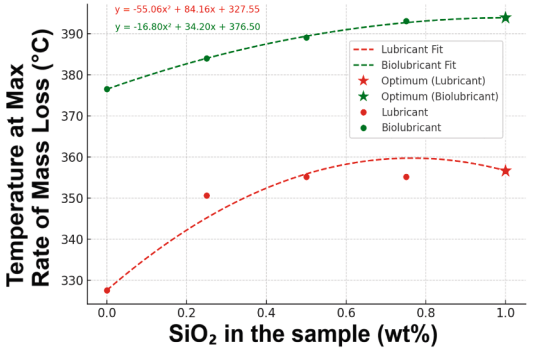

(h)

Fig. 3. Comparative thermogravimetric analysis and derivative parameters of lubricants (red curves) and biolubricants (green curves) as a function of SiO_2 nanoparticles percentage in the formulation, obtained by TGA at 5.5 K·min^{-1} under nitrogen atmosphere: (a) onset temperature, (b) midpoint temperature, (c) inflection temperature, (d) end temperature, (e) mass change, (f) residual mass, (g) maximum rate of mass loss, (h) temperature at maximum degradation rate.

Table 6
TGA and DTG results for formulations based on the conventional lubricant (average ± one standard deviation).

SiO_2 in the sample (wt%)	Onset t. (°C)	Midpoint t. (°C)	Inflection t. (°C)	End t. (°C)	Mass Change (%)	Residual Mass (%)	Rate of mass loss (%·min^{-1})	FWHM (°C)
0.00	272.95 ± 0.64	314.1 ± 1.41	327.1 ± 6.51	359.1 ± 2.40	−83.81 ± 0.83	0.0 ± 0.00	−5.94 ± 0.05 at 327.55 ± 3.18 °C	66.15 ± 3.98 °C
0.25	294.6 ± 0.00	335.95 ± 0.49	353.35 ± 4.88	385.05 ± 1.48	−80.69 ± 0.51	0.89 ± 0.27	−5.62 ± 0.01 at 350.65 ± 1.77 °C	80.04 ± 1.61 °C
0.50	296.7 ± 2.97	337.9 ± 3.25	352.55 ± 3.75	387.85 ± 5.44	−80.16 ± 1.26	1.16 ± 0.11	−5.5 ± 0.16 at 355.15 ± 4.60 °C	82.81 ± 5.52 °C
0.75	295.5 ± 0.99	337.2 ± 0.71	349.35 ± 1.06	387.5 ± 0.57	−80.0 ± 0.24	1.86 ± 1.19	−5.46 ± 0.01 at 355.15 ± 0.35 °C	82.06 ± 2.51 °C
1.00	297.5 ± 1.84	338.95 ± 1.77	352.65 ± 3.61	389.8 ± 2.69	−79.55 ± 0.40	1.96 ± 1.04	−5.42 ± 0.04 at 356.65 ± 2.47 °C	83.50 ± 4.55 °C

Table 7
TGA and DTG results for formulations based on the biolubricant (average ± one standard deviations).

SiO_2 in the sample (wt%)	Onset t. (°C)	Midpoint t. (°C)	Inflection t. (°C)	End t. (°C)	Mass Change (%)	Residual Mass (%)	Rate of mass loss (%·min^{-1})	FWHM (°C)
0.00	321.6 ± 6.24	352.2 ± 5.51	374.3 ± 4.31	390.9 ± 5.44	−86.42 ± 0.01	1.56 ± 0.07	−7.62 ± 0.19 at 376.5 ± 6.22 °C	40.70 ± 0.60 °C
0.25	331.6 ± 7.86	360.4 ± 6.07	383.3 ± 8.49	397.7 ± 4.02	−86.77 ± 0.50	2.23 ± 0.88	−8.06 ± 0.45 at 384.0 ± 4.38 °C	36.07 ± 2.21 °C
0.50	339.0 ± 2.68	366.2 ± 2.13	390.9 ± 2.34	401.6 ± 1.48	−87.11 ± 0.01	2.58 ± 0.39	−8.52 ± 0.20 at 389.1 ± 2.69 °C	39.81 ± 3.08 °C
0.75	343.9 ± 4.24	370.8 ± 4.38	392.3 ± 0.49	404.8 ± 3.04	−86.92 ± 0.26	2.29 ± 0.01	−8.72 ± 0.08 at 393.1 ± 2.83 °C	42.69 ± 0.99 °C
1.00	345.3 ± 0.64	372.4 ± 0.21	390.7 ± 1.70	405.7 ± 0.14	−86.88 ± 1.05	2.37 ± 0.22	−8.60 ± 0.07 at 393.9 ± 2.12 °C	40.45 ± 3.33 °C

$$y = -16.80 \cdot x^2 + 34.20 \cdot x + 376.50 \text{ (biolubricant)} \quad (10)$$

Optimum T_{max} was reached around 0.76 wt% for lubricant and ~ 1.00 wt% for biolubricant (NB: also in this case, the upper mass-percentage limit was indicated, as the vertex is placed outside the inquired interval). To further quantify degradation-rate narrowing or widening, the DTG peak full width at half maximum (FWHM) was extracted from temperature-based DTG curves (Table 6 and Table 7). For conventional lubricants, FWHM increased markedly from 66.15 ± 3.98 °C (neat oil) to ~ 80–83 °C for SiO_2-containing formulations, indicating a broader DTG peak and a more distributed degradation process. In contrast, biolubricants showed comparatively narrower DTG peaks overall (~36–43 °C), with no systematic broadening, while exhibiting higher max mass-loss rate and higher T_{max}. Combined, T_{max}, maximum degradation rate, and FWHM support the interpretation of slower, more distributed degradation in mineral oil and delayed yet more intense degradation in biolubricants once decomposition initiates.

These results indicate that the organic matrix in the biolubricants degrades more quickly at higher temperatures due to oxidation, and that the addition of nanoparticles (spec. SiO_2 nanoparticles) can enhance thermal stability and postpone this decomposition. Most parameters show a plateau or diminishing returns beyond 0.75–1.00 wt% SiO_2, suggesting that this range is mostly optimal for maximizing thermal performance while avoiding excessive additive loading. This evidence is fully consistent with prior findings on antioxidant-charged biolubricant formulations [61,62].

Oxidation resistance analysis

Lubricant oxidation contributes to the corrosion of non-ferrous metals and the formation of deposits. It can also lead to sludge buildup, corrosive acid formation, and oil viscosity increase [63]. DSC can detect exothermic transitions, such as oxidation, thus providing valuable insights into the process [27,29,60]. Therefore, by comparing the enthalpies associated with these exothermic transitions, observed via DSC, the influence of SiO_2 nanoparticles on the oxidation behavior of lubricants and biolubricants can be effectively analyzed.

Oxidation resistance of lubricants and biolubricants with and without SiO_2 nanoparticles is highlighted by the DSC results reported in Fig. 4 for the lubricant and the biolubricant formulations at different wt % of SiO_2 nanoparticles. Fig. 5 presents the comparative DSC analysis of lubricants and biolubricants enhanced with SiO_2 nanoparticles, and Table 8 and Table 9, summarized the DSC results.

Multiple oxidation peaks can be seen in biolubricants, which implies that the lubricant matrix's various constituents oxidize at various temperatures [64]. In this study, the lower-temperature exothermic feature (P1) is tentatively attributed to the oxidation of ester-based base oil components, while the higher-temperature feature (P2) is associated with additive and antioxidant-related oxidation processes, in agreement with previous reports on ester-containing lubricants. Under the present experimental conditions, these exothermic features originate from oxidative reactions arising from residual oxygen diffusion through the pierced crucible during dynamic DSC measurements conducted under nitrogen purge, rather than from a controlled oxygen-rich atmosphere. The incorporation of additives, such as SiO_2 nanoparticles, does not introduce new reactants into the system; instead, these nanoparticles interact physically with the lubricant matrix, influencing heat transfer, oxygen diffusion, and the stability of intermediate oxidation species. As a result, the oxidation pathways may be redistributed, leading to shifted or multiple overlapping oxidation peaks in the DSC curves [29,30,65,66].

DSC results clearly demonstrate that nanoparticle-charged lubricants and biolubricants exhibit increased resistance to oxidation. Indeed, both enthalpy and oxidation induction time (OIT) values increased by increasing SiO_2 nanoparticles concentration.

Although SiO_2 nanoparticles do not act as reactants in the oxidation process, their presence can significantly influence the oxidation pathway and product distribution by affecting heat transfer, oxygen diffusion, and interactions with intermediate oxidation species within the lubricant matrix. Consequently, the observed changes in oxidation enthalpy are not attributed to a simple acceleration of the same reaction, but rather to a redistribution of overlapping oxidation reactions and the

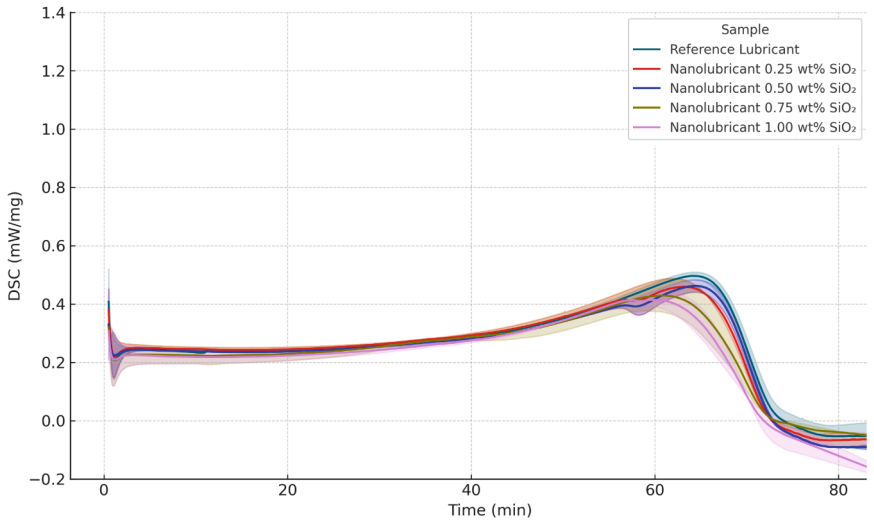

(a)

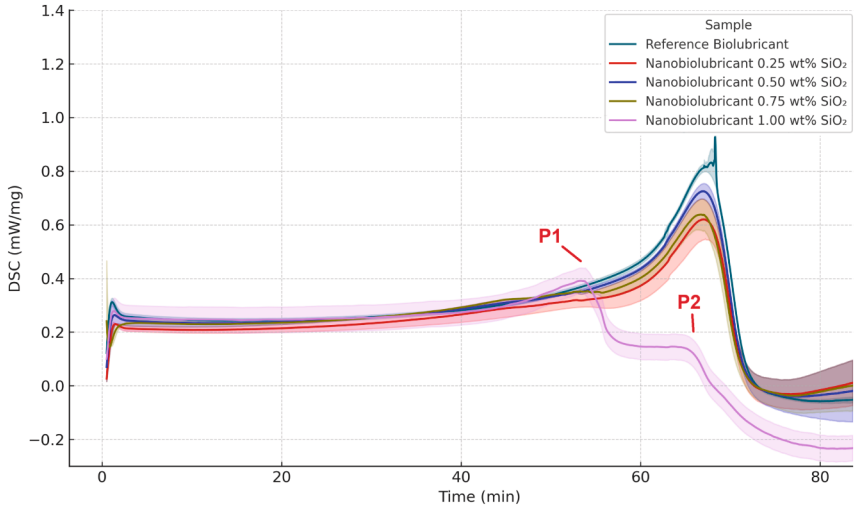

(b)

Fig. 4. DSC plots of Nanolubricants (a) and Nanobiolubricants (b) obtained under dynamic heating conditions (5.5 K·min^{-1}) from 40 °C to 500 °C under nitrogen purge (100 mL·min^{-1}). In both the plots, the central curves represent the average trends and the surrounding shaded areas the dispersion of experimental values calculated in correspondence to one standard deviation (n = 2). Multiple exothermic peaks (P1 and P2) are highlighted, corresponding to overlapping oxidation-related processes occurring during thermal degradation.

formation of oxidation products with different enthalpic contributions. Therefore, the large variation in enthalpy reflects a change in oxidation mechanisms rather than a contradiction of thermodynamic principles.

The lowest oxidation resistance was registered by pure lubricants, associated with the shortest OIT of 20.70 ± 0.14 min and lowest enthalpy of 280.2 ± 8.34 J·g^{-1} (Table 8).

The best results were obtained with 0.75 wt% SiO_2 and 1.00 wt% SiO_2, associated to the longest OIT values of 25.6 ± 0.94 min and 27.70 ± 1.04 min and the highest enthalpy values of 413.6 ± 9.15 J·g^{-1} and 459.85 ± 12.66 J·g^{-1}, respectively (Table 8).

Pure biolubricant exhibits a considerably lower oxidation resistance than pure conventional lubricant, with an OIT of just 6.6 ± 1.7 min and an enthalpy value of 201.25 ± 5.3 J·g^{-1} (Table 9). Similarly, the oxidation resistance of biolubricants is greatly increased by the addition of SiO_2 nanoparticles. The OIT increases by approximately 45% up to the value of 9.55 ± 0.64 min at 0.25 wt% SiO_2, and enthalpy rises sharply to 299.55 ± 13.93 J·g^{-1} (Table 9). With the highest enthalpy values (429.95 ± 43.2 J·g^{-1} and 509.45 ± 26.8 J·g^{-1}) and the longest OITs (20.2 ± 0.28 min and 29.65 ± 3.18 min), the samples with 0.75 wt% SiO_2 and 1.00 wt% SiO_2, respectively (Table 9), show the most significant improvements [29,30].

Polynomial fitting of the DSC parameters shows strong correlation with SiO_2 content ($R^2 > 0.98$). The fitted equations for OIT were

$$y = -1.15 \cdot x^2 + 8.15 \cdot x + 20.70 \text{ (lubricant)} \quad (11)$$

$$y = +25.32 \cdot x^2 - 2.27 \cdot x + 6.60 \text{ (biolubricant)} \quad (12)$$

Estimating optimal OIT at ~ 1.00 wt% for lubricant (NB: the vertex is at 3.54 in this case, hence outside the inquired interval, so the upper limit was indicated) and ~ 1.00 wt% for biolubricant (the upper limit also in this case), due to the increasing trend of the curve. Enthalpy showed a similar trend:

$$y = +53.20 \cdot x^2 + 126.45 \cdot x + 280.20 \text{ (lubricant)} \quad (13)$$

$$y = +63.72 \cdot x^2 + 244.48 \cdot x + 201.25 \text{ (biolubricant)} \quad (14)$$

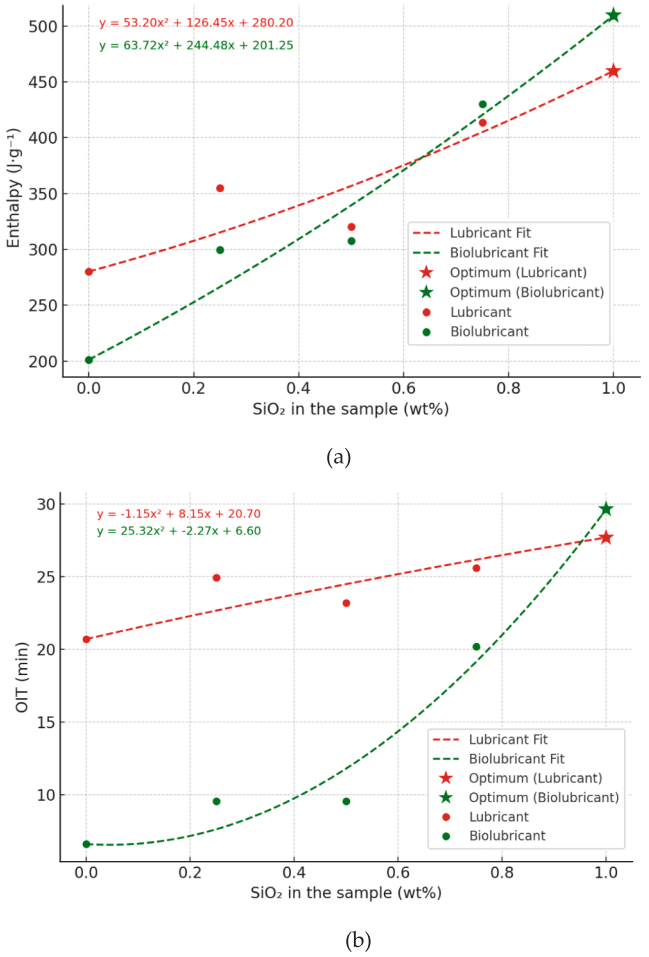

Fig. 5. Comparative differential scanning calorimetry analysis of lubricants (red curves) and biolubricants (green curves) as a function of SiO_2 nanoparticles percentage in the formulation: (a) enthalpy, (b) oxidation induction time.

Table 8
DSC results for formulations based on the conventional lubricant (average ± one standard deviation). Enthalpy values were obtained from dynamic DSC scans (40–500 °C, 5.5 K·min^{-1}) under nitrogen purge (100 mL·min^{-1}). OIT values were determined from the same DSC thermograms and defined as the time-to-onset of the main exothermic oxidation peak using the Proteus onset criterion.

SiO_2 in the sample (wt%)	Enthalpy (J·g^{-1})	OIT (min)
0.00	280.20 ± 8.34	20.70 ± 0.14
0.25	355.00 ± 10.85	24.95 ± 0.82
0.50	320.35 ± 12.23	23.20 ± 0.99
0.75	413.60 ± 9.15	25.60 ± 0.94
1.00	459.85 ± 12.66	27.70 ± 1.04

Table 9
DSC results for formulations based on the biolubricants (average ± one standard deviation). Enthalpy values were obtained from dynamic DSC scans (40–500 °C, 5.5 K·min^{-1}) under nitrogen purge (100 mL·min^{-1}). OIT values were determined from the same DSC thermograms and defined as the time-to-onset of the main exothermic oxidation peak using the Proteus onset criterion.

SiO_2 in the sample (wt%)	Enthalpy (J·g^{-1})	OIT (min)
0.00	201.25 ± 5.30	6.60 ± 1.70
0.25	299.55 ± 13.93	9.55 ± 0.64
0.50	307.40 ± 16.97	9.55 ± 0.64
0.75	429.95 ± 43.20	20.20 ± 0.28
1.00	509.45 ± 26.8	29.65 ± 3.18

Yielding optimal enhancement at ~ 1.00 wt% for both types, thanks to the increasing trend of these curves with the increasing of the mass percentage of nanoparticles. These trends confirm that oxidation resistance benefits a lot from SiO_2 addition, especially at higher concentrations (in this case: approaching 1.00 wt%).

From an application perspective, an SiO_2 loading in the range of 0.75–1.00 wt% provides the most balanced improvement across oxidation induction time and enthalpy metrics.

Benchmarking thermal and oxidation performance against the literature

A comparison with existing studies can underscore the exceptional performance of the KH570–SiO_2–biolubricant system developed in this work. For instance, Abdul Khaliq Rasheed et al. [28] reported a 13–17 °C increase in oxidation onset temperature for mineral lubricants modified with graphene, and Maheswaran et al. [29] observed a 100 °C improvement in decomposition temperature for nano-garnet–enhanced SN500 oil. In contrast, the KH570–SiO_2–biolubricant achieved an onset temperature rise of 23.7 °C, accompanied by an approximately 2.5-fold increase in enthalpy and a 4.5-fold increase in OIT at 1.00 wt% nanoparticle loading. Similarly, NiO nanoparticles in SN500 lubricants [30] eliminated mass loss at 200 °C at particle-charges of up to 0.3 wt%, and Al_2O_3/TiO_2 hybrids [31,67] improved the onset temperature by up to 54.9 °C, yet these systems generally reported lower OIT gains compared to the KH570–SiO_2 formulation. Recent works with graphene/maghemite [32], CdS/Co_3O_4 [68], and MoS_2-based hybrids [69–72] demonstrated notable oxidation delay and thermal resistance, often peaking at specific loadings before declining due to agglomeration, an effect not observed within the concentration range tested in this study. Moreover, ZnO-based [73] and MXene-based [74] systems achieved moderate OIT improvements (up to ~ 54.8%), but without the simultaneous, balanced gains in thermal stability, enthalpy, and oxidation resistance observed here.

Collectively, these comparisons position the KH570–SiO_2–biolubricant formulation as a benchmark for high-performance biolubricant design in terms of both thermal degradation resistance and oxidation delay.

Beyond the quantitative benchmarking summarized in Table 10, the superior thermal and oxidation performance of the KH570–SiO_2–biolubricant system can be rationalized by several complementary physicochemical mechanisms. First, well-dispersed SiO_2 nanoparticles may act as radical scavengers and physical barriers, hindering oxygen diffusion and slowing chain-propagation reactions during oxidation. Second, the KH570 silane shell enhances interfacial compatibility between the inorganic nanoparticles and the oil matrix, promoting more homogeneous dispersion and more efficient heat dissipation under thermal load. At higher nanoparticle contents (~ 0.75–1.00 wt%), dilution and heat-sink effects become dominant, leading to diminishing returns or plateau behavior in several thermal metrics. Importantly, the absence of pro-oxidant metal species—confirmed by ICP-OES analyses in our previous work—excludes catalytic oxidation pathways, supporting that the observed trends are intrinsic to the SiO_2-based formulation. These mechanistic interpretations are further consistent with the enhanced TBN retention and moderated TAN increase reported in Tables 4–5 as a function of nanoparticle loading.

Conclusions

The potential of nanoparticles as an additive has emerged as a promising strategy in the search for innovative lubricants able to withstand both the oxidative stress and the high temperatures. This work aimed to ascertain if SiO_2 nanoparticles coated with KH570-Silane coupling agent could have enhanced lubricant resistance to oxidation and thermal stability. The TGA and DTG analysis confirmed that SiO_2

Table 10
Comparative summary of nanoparticle effects on thermal stability and oxidation resistance improvements in lubricants and biolubricants.

Ref	Lubricant Type	Nanoparticle	Concentration (s)	Analysis Technique	Onset Temp (°C)	Enthalpy ($J \cdot g^{-1}$)	OIT (min)	Notes
This study	Biolubricant (PLANTO MOT SAE 10W40)	KH570-SiO_2 (18–35 nm)	0.25, 0.50, 0.75, and 1.00 wt%	TGA,DTG, DSC	Base: 321.60 ± 6.24; (1.00 wt%): 345.30 ± 0.64	Base: 201.25 ± 5.30 (1.00 wt%): 509.45 ± 26.80	Base: 6.60 ± 1.70 (1.00 wt %): 29.65 ± 3.18	Improved stability and oxidation resistance;
This study	lubricant (Mistral 15W40)	KH570-SiO_2 (18–35 nm)	0.25, 0.50, 0.75, and 1.00 wt%	TGA,DTG, DSC	Base: 272.95 ± 0.64; With NP: 297.50 ± 1.84	Base: 280.20 ± 8.34 (1.00 wt%): 459.85 ± 12.66	Base: 20.70 ± 0.14 (1.00 wt%): 27.70 ± 1.04	Improved stability and oxidation re-sistance;
Abdul Khaliq Rasheed et al. (2015) [28]	Mineral lubricants (20W50 SN/CF and 20W50 SJ/CF)	Graphene flakes (8, 12, and 60 nm thick)	0.01 wt%	TGA	Base: 297.79; G8 nm: 310.80; G12 nm: 312.90; G60 nm: 314.80	n/r	n/r	Graphene improved thermal stability; higher onset temperature; reduced activation energy.
Maheswaran et al. (2016) [29]	Mineral oil (SN500, EP grade)	Nano-garnet (~45 nm)	0.25 and 0.75 wt %	TGA, DSC	Base: 175; (0.25 wt%): 275; (0.25 wt%): 240	n/r	n/r	Improved heat resistence
Ramachandran et al. (2018) [30]	Base oil lubricant (SN500)	NiO nanopar (~50 nm)	0.10, 0.30 and 0.50 wt%	TGA,DTG, DSC	Base: 42; (0.10 wt%): 204; (0.30 wt%): 208 (0.50 wt%): 70	Base: 184.80 (0.50 wt%): 237.20	n/r	Thermal stability increased with NiO addition up to 0.30 wt%, then decreased due to agglomeration
Mohamed Kamal et al. (2019) [31]	Lubricant (Castrol EDGE professional A5 5W30)	Al_2O_3 (8–12 nm) andTiO_2 (10 nm)	0.10 wt%	TGA,DTG, DSC	Base: 245.60; With NP: 300.5	n/r	n/r	Improved thermal stability and oxidation resistance
Mohamed Kamal et al. (2020) [67]	PAO6 + 5 wt% HDEHP	Al_2O_3/TiO_2 (25–30 nm)	0.10 wt%	TGA	Base: 251 With NP: 275	n/r	n/r	Improved thermal stability and oxidation resistance
Ibrahim Ogu Sadiq et al. (2022) [32]	Coconut oil	Graphene (xGNP) (≈ 6–8 nm) and Maghemite (γ-Fe_2O_3) (≈ 9.5 nm)	0.10 vol%	TGA	Base: 325.00 (MGCO): 343.75 (XGCO): 362.50	n/r	n/r	For (XGCO), Onset delayed by 37.50 °C; 35% weight loss at 387 °C; best thermal stability
Muhammad Fasehullah et al. (2022) [68]	Synthetic ester (Midel-7131 insulating oil)	CdS (≈ 10 nm) and Co_3O_4 (≈ 20 nm)	CdS: (0.30 $g \cdot L^{-1}$); Co_3O_4: (0.05 $g \cdot L^{-1}$)	TGA,DTG, DSC	Base: 334.20; CdS: 334.43; Co_3O_4: 335.26	Base: 469.51; CdS: 408.15; Co_3O_4: 405.82	n/r	Nanofluids showed slightly higher onset temperatures than base oil, indicating improved thermal stability; enthalpy values lower than base oil.
Thachnatharen Nagarajan et al. (2022) [69]	Lubricant (SAE 20W50)	MoS_2 (150–300 nm)	0.005, 0.01, 0.05 and 0.10 wt%	DSC	n/r	n/r	Base: 18.70; 0.005 wt %: 23.50; 0.01 wt%: 30.10; 0.05 wt%: 31.00; 0.10 wt%: 20.90	Highest OIT improvement by 65.68% (0.05 wt%), for 0.01 lower stability due to agglomeration
Thachnatharen Nagarajan et al. (2023) [70]	Lubricant (SAE 20W40)	MoS_2–Graphene nanohybrid	0.005, 0.01, 0.05, and 0.10 wt%	DSC	n/r	n/r	Base: 25; 0.05 wt%: 29.80	OIT peaked at 0.05 wt% (+19.21%), decreased at higher loadings due to agglomeration
Thachnatharen Nagarajan et al. (2023) [51]	Lubricant (SAE 20W40)	MoS_2–hBN hybrid	0.005, 0.01, 0.05, and 0.10 wt%	DSC	n/r	n/r	Base: 25; 0.05 wt%: 33	OIT peaked at 0.05 wt% MoS_2–hBN (+38.76%)
Kalaimani Markandan et al. (2023) [72]	Lubricant (SAE 5W40)	MoS_2-Ti_3C_2 MXene (functionalized and unfunctionalized)	0.01 and 0.05 wt %	DSC	n/r	n/r	Base: 44.50; 0.01 wt%: 52.50;	The highest OIT was for 0.01 wt% functionalized MoS_2/MXene (~52.50 min),
Marta Hernaiz et al. (2023) [73]	Formulated synthetic lubricant	ZnO (20 nm) and OA-functionalized ZnO	0.10, 0.50, and 1.00 wt %	DSC	n/r	n/r	Base: 49 ± 0.50; F-ZnO-Group II (0.01 wt	OA alone lowered OIT vs reference; best OIT at 1.00 wt% F-ZnO-Group II (+19.80% vs ref).

(*continued on next page*)

Table 10 (*continued*)

Ref	Lubricant Type	Nanoparticle	Concentration (s)	Analysis Technique	Onset Temp (°C)	Enthalpy ($J \cdot g^{-1}$)	OIT (min)	Notes
Haizum Aimi Zaharin et al. (2023) [74]	Outboard lubricant (TC-W)	$Ti_3C_2T_x$ MXene	0.005, 0.01, 0.05 wt%	DSC	n/r	n/r	%): 59 ± 0.50 Base: 12.90; 0.01%: 20.00	0.01 wt% gave optimal performance for OIT (+54.80%)

nanoparticles dramatically increase the thermal stability of lubricants and biolubricants, while via DSC, the oxidation resistance and the oxidation induction time were examined. Based on the observation of stabilization plateaus and diminishing returns at higher nanoparticle contents, an SiO_2 concentration in the range of 0.75–1.00 wt% can be identified as an optimal operating window for enhancing thermal and oxidative endurance in both lubricant and biolubricant formulations. While the findings highlight the promising properties of nanolubricants/nanobiolubricants, further research is needed to evaluate their performance under real-world conditions, characterized by non-constant operative temperatures and by the presence of contaminating agents (e.g. fuels, combustion residues, etc. in internal combustion engines). In this context, fuel dilution represents a particularly critical challenge for conventional lubricants, particularly as biofuels gain increasing attention and are more prone to penetrate and dilute the lubricant during engine operation.

Despite the promising results reported in this study, several limitations should be acknowledged. The present investigation was conducted under controlled laboratory conditions using thermogravimetric and calorimetric techniques, which, although effective for isolating thermal and oxidative phenomena, do not fully replicate the complex and dynamic conditions encountered in real engine operation. In addition, tribological performance, long-term field aging, regeneration or reusability of the biolubricant, and multi-cycle degradation behavior were beyond the scope of this work. Furthermore, the statistical evaluation is based on duplicate measurements, which provides an estimate of repeatability but does not capture broader population variability.

Building on the results obtained in this study, several future research directions can be identified. The demonstrated improvements in thermal stability, oxidation resistance, and oxidation induction time suggest that KH570–SiO_2 nanoparticles may enable extended service intervals and improved durability of biolubricants under demanding operating conditions.

It should also be acknowledged that oxidation induction time (OIT) measurements were performed under controlled DSC conditions, employing an inert nitrogen purge and a pin-holed crucible with defined oxygen exposure. While this approach enables reproducible comparison of oxidative stability, it does not fully reproduce the complex oxidative environments encountered in real engine operation. Accordingly, future investigations will consider air- and O_2-based DSC protocols, as well as engine-aging tests, to further validate the observed trends under realistic operating conditions.

Future studies should therefore focus on validating these findings under real engine environments, including variable load, temperature cycling, and fuel contamination effects. In addition, long-term aging and multi-cycle testing would be valuable to assess the persistence of the observed stabilization effects over prolonged use. The influence of KH570–SiO_2 nanoparticles on tribological performance, friction reduction, and wear behavior also warrants systematic investigation. Finally, optimization of nanoparticle loading for different base oil chemistries, together with assessments of regeneration and reusability strategies, could further enhance the practical applicability and sustainability of nanoparticle-enhanced biolubricant formulations.

These approaches would provide deeper insights into the nanoparticles' behavior and potential benefits in industrial and automotive applications and, therefore, in the authors' intentions, both should be considered.

CRediT authorship contribution statement

Homeyra Piri: Writing – review & editing, Writing – original draft, Visualization, Validation, Resources, Methodology, Investigation, Formal analysis, Data curation, Conceptualization. **Vittoria Benedetti:** Writing – review & editing, Validation, Methodology, Formal analysis, Conceptualization. **Salar Moradi:** Validation, Investigation, Conceptualization. **Massimiliano Renzi:** Writing – review & editing, Validation, Supervision, Conceptualization. **Marco Bietresato:** Writing – review & editing, Validation, Supervision, Conceptualization.

Funding

This research received no external funding.

Declaration of competing interest

The authors declare that they have no known competing financial interests or personal relationships that could have appeared to influence the work reported in this paper.

Acknowledgments

The authors wish to thank: Dott. Ivo Cordioli for his useful suggestions about lubricants, and the company management of NILS S.p.A. (Postal, Bolzano, Italy), for letting Homeyra Piri be hosted for an 8-month internship period, thus allowing her to develop a proper expertise about lubricants. The authors wish also to thank NILS S.p.A and FUCHS LUBRICANTS GERMANY GmbH for having provided the lubricant and biolubricant used in the tests free of charge.

Data availability

The raw data supporting the conclusions of this article will be made available by the authors on request.

References

[1] K. Holmberg, P. Andersson, and A. Erdemir, 'Global energy consumption due to friction in passenger cars', *Tribol Int*, vol. 47, 2012, doi: 10.1016/j.triboint.2011.11.022.
[2] H. Spikes, 'Friction Modifier Additives', *Tribol Lett*, vol. 60, no. 1, Oct. 2015, doi: 10.1007/s11249-015-0589-z.
[3] M. Gulzar *et al.*, 'Tribological performance of nanoparticles as lubricating oil additives', Aug. 01, 2016, *Springer Netherlands*. doi: 10.1007/s11051-016-3537-4.
[4] L. Duan, J. Li, and H. Duan, 'Nanomaterials for lubricating oil application: A review', May 01, 2023, *Tsinghua University*. doi: 10.1007/s40544-022-0667-9.
[5] Vincent Gatto, 'The chemistry and function of lubricant additives'. Accessed: Mar. 25, 2024. [Online]. Available: https://www.stle.org/images/pdf/STLE_ORG/BOK/LS/Additives/The%20Chemistry%20and%20Function%20of%20Lubricant%20Additives.pdf.
[6] H. Piri, C. Caligiuri, M. Brolpasino, M. Renzi, and M. Bietresato, 'Biolubricant ageing analysis: Proposal for a real-engine test and chemical characterization', *Journal of the Energy Institute*, vol. 121, p. 102121, Aug. 2025, doi: 10.1016/j.joei.2025.102121.
[7] Wang P, Wang Y, Sun Y, Cao Z, Zhu W, Wang H. Thermal and Spectroscopic Studies of the Thermal-Oxidation Stabilities of Lubricants. J Appl Spectrosc Sep. 2021;88 (4):847–54. https://doi.org/10.1007/s10812-021-01249-6.

[8] C. Murru, R. Badía-Laíño, and M. E. Díaz-García, 'Oxidative Stability of Vegetal Oil-Based Lubricants', Feb. 01, 2021, *American Chemical Society*. doi: 10.1021/acssuschemeng.0c06988.

[9] R. Uppar, P. Dinesha, and S. Kumar, 'A critical review on vegetable oil-based bio-lubricants: preparation, characterization, and challenges', Sep. 01, 2023, *Springer Science and Business Media B.V.* doi: 10.1007/s10668-022-02669-w.

[10] Roy M. Mortier, Malcolm F. Fox, and Stefan T. Orszulik, *Chemistry and Technology of Lubricants*. Springer Netherlands, 2010. doi: doi:10.1007/978-1-4020-8662-5.

[11] Leslie R. Rudnick, 'Lubricant Additives: Chemistry and applications. Third Edition' 2017. https://doi.org/10.1201/9781315120621.

[12] Johnson DW. 'Turbine Engine Lubricant and Additive Degradation Mechanisms', in *Aerospace Engineering*. IntechOpen 2019. https://doi.org/10.5772/intechopen.82398.

[13] P. M. Lee *et al.*, 'Lubricant Degradation, Transport and the effect of extended oil drain intervals on Piston Assembly Tribology', 2006.

[14] Fox NJ, Stachowiak GW. Vegetable oil-based lubricants-a review of oxidation. Tribol Int Jul. 2007;40(7):1035–46. https://doi.org/10.1016/j.triboint.2006.10.001.

[15] 'Additives in Motor Oil: Everything You Need to Know'. Accessed: Jul. 27, 2025. [Online]. Available: https://blog.amsoil.com/more-than-you-ever-wanted-to-know-about-motor-oil-additives/#:~:text=Additives%20in%20motor%20oil%20themselves,negative%20effects%20additives%20may%20cause.

[16] 'Understanding Lubricant Physical Properties and Chemistry'. Accessed: Jul. 30, 2025. [Online]. Available: https://www.jetlube.com/blog/understanding-lubricant-physical-properties-and-chemistry#:~:text=Detergents%20have%20their%20disadvantages,only%20used%20in%20limited%20applications.

[17] 'Lubricant Additives - A Practical Guide'. Accessed: Jul. 27, 2025. [Online]. Available: https://www.machinerylubrication.com/Read/31107/oil-lubricant-additives#:~:text=They%20can%20be%20corrosive%20toward,used%20due%20to%20corrosion%20concerns.

[18] 'Additives and engine oil lubrication'. Accessed: Jul. 30, 2025. [Online]. Available: https://www.plantengineering.com/additives-and-engine-oil-lubrication/.

[19] 'Controlling Oil Aeration and Foam'. Accessed: Jul. 30, 2025. [Online]. Available: https://www.machinerylubrication.com/Read/255/oil-foam#:~:text=Alkaline%20detergents%20can%20react%20with,seems%20to%20control%20their%20effects.

[20] 'Limitations of Extreme Pressure Additives'. Accessed: Jul. 30, 2025. [Online]. Available: https://www.machinerylubrication.com/Read/29031/extreme-pressure-additives#:~:text=5.%C2%A0%20Sulfur,these%20oils%20can%20be%20used.

[21] Bietresato M, Friso D. Durability test on an agricultural tractor engine fuelled with pure biodiesel (B100). Turk J Agric For 2014;38(2):214–23. https://doi.org/10.3906/tar-1302-51.

[22] 'A Beginner's Guide to Thermogravimetric Analysis'. Accessed: Nov. 19, 2024. [Online]. Available: https://www.xrfscientific.com/beginners-guide-thermogravimetric-analysis/.

[23] 'Thermogravimetry Differential Thermal Analysis (TG/DTA)'. Accessed: Nov. 19, 2024. [Online]. Available: https://www.eag.com/techniques/phys-chem/thermogravimetry-differential-thermal-analysis-tg-dta/.

[24] 'Oxidation Induction Time Measurements by DSC'. Accessed: Aug. 23, 2025. [Online]. Available: https://www.hitachi-hightech.com/file/global/pdf/products/science/appli/ana/thermal/application_TA_049e.pdf.

[25] R. I. M. Almoselhy, 'Applications of Differential Scanning Calorimetry (DSC) in Oils and Fats Research. A Review', *American Research Journal of Agriculture*, vol. 6, no. 1, pp. 1–9, Dec. 2020, doi: 10.21694/2378-9018.20002.

[26] Ghanbari E, Picken SJ, van Esch JH. Analysis of differential scanning calorimetry (DSC): determining the transition temperatures, and enthalpy and heat capacity changes in multicomponent systems by analytical model fitting. J Therm Anal Calorim Nov. 2023;148(22):12393–409. https://doi.org/10.1007/s10973-023-12356-1.

[27] R. Natalia, C. Pardo, G. Miriam, A. Rojas, and L. M. Florez, 'Thermal analysis of the physicochemical properties of organic waste to application in the compost process', doi: 10.1007/s13399-021-01786-2/Published.

[28] A. K. Rasheed, M. Khalid, W. Rashmi, T. C. S. M. Gupta, and A. Chan, 'Study of graphene nanolubricant using thermogravimetric analysis', 2015. doi: 10.1557/jmr.2015.359.

[29] Maheswaran R, Sunil J. Effect of nano sized garnet particles dispersion on the viscous behavior of extreme pressure lubricant oil. J Mol Liq Nov. 2016;223:643–51. https://doi.org/10.1016/j.molliq.2016.08.106.

[30] K. Ramachandran, P. Navaneethakrishnan, and M. Sivaraja, 'The Influence of Nickel Oxide Nanoparticle Dispersion on the Thermo Stability of Lubricant Oil', *Int J Nanosci*, vol. 19, no. 1, Feb. 2020, doi: 10.1142/S0219581X18500448.

[31] Ali MKA, Xianjun H. Improving the heat transfer capability and thermal stability of vehicle engine oils using Al2O3/TiO2 nanomaterials. Powder Technol Mar. 2020;363:48–58. https://doi.org/10.1016/j.powtec.2019.12.051.

[32] I. O. Sadiq, M. A. Suhaimi, S. Sharif, N. Mohd Yusof, and M. J. Hisam, 'Enhanced performance of bio-lubricant properties with nano-additives for sustainable lubrication', *Industrial Lubrication and Tribology*, vol. 74, no. 9, pp. 995–1006, Oct. 2022, doi: 10.1108/ILT-08-2021-0348.

[33] M. F. Ismail and W. A. Wan Hamzah, 'Tribological Performance Effect of SiO2 and TiO2 Nanoparticles as Lubricating Oil Additives', in *Lecture Notes in Mechanical Engineering*, Springer Science and Business Media Deutschland GmbH, 2023, pp. 223–231. doi: 10.1007/978-981-19-4425-3_20.

[34] H. H. Patil, 'Tribological Properties Of Sio 2 Nanoparticles Added In SN-500 Base Oil'. [Online]. Available: www.ijert.org.

[35] A. A. K, 'Tribological Behavior and Performance of Lubricants Filled with Nanoparticles: A Review', *American Journal of Engineering Research (AJER)*, vol. 10, pp. 230–236, [Online]. Available: www.ajer.org.

[36] Theo M, Wilfried D. 'Lubricants and Lubrication', in *Lubricants and Lubrication*. Wiley 2017. https://doi.org/10.1002/9783527645565.fmatter.

[37] P. R. Bod1, P. Protim Borthakur, E. Baruah, R. Deka, and S. Kerolina, 'A Review of Properties, Synthesis Procedure, Characterization and Application for Silicon Oxide Nanoparticles'.

[38] D. K. Ferry and D. L. Rode, 'Physical and electrical properties of silica', 2025. doi: 10.1063/5.0233576.

[39] Reed ML, Fedder GK. 2. Photolithographic microfabrication. Handbook of Sensors and Actuators 1998;6:13–61. https://doi.org/10.1016/S1386-2766(98)80003-0.

[40] A. Abdelazim, M. Taha, A. Rashed, A. Nabhan, and R. Khiari, 'Sustainable Nanoparticles in Lubrication System: A Review of Eco-Friendly and Inorganic Additives'. [Online]. Available: https://www.jacs-dz.org.

[41] Shen C, Wang H, Zhang T, Zeng Y. Silica coating onto graphene for improving thermal conductivity and electrical insulation of graphene/polydimethylsiloxane nanocomposites. J Mater Sci Technol Jan. 2019;35(1):36–43. https://doi.org/10.1016/j.jmst.2018.09.016.

[42] Piri H, Renzi M, Bietresato M. Enhancing Performance and Sustainability of Engine Lubricants and Biolubricants by Dispersing SiO2 Nanoparticles Coated with KH570-Silane Coupling Agent. Appl Sci Sep. 2024;14(17):7943. https://doi.org/10.3390/app14177943.

[43] Dhand V, Rhee KY, Ju Kim H, Ho Jung D. A comprehensive review of graphene nanocomposites: Research status and trends. J Nanomater 2013, 2013,. https://doi.org/10.1155/2013/763953.

[44] Y. Cui, S. I. Kundalwal, and S. Kumar, 'Gas Barrier Performance of Graphene/Polymer Nanocomposites'.

[45] T. D. F. López, A. F. González, Á. Del Reguero, M. Matos, M. E. Díaz-García, and R. Badía-Laíño, 'Engineered silica nanoparticles as additives in lubricant oils', *Sci Technol Adv Mater*, vol. 16, no. 5, 2015, doi: 10.1088/1468-6996/16/5/055005.

[46] P. Uniyal, P. Gaur, J. Yadav, T. Khan, and O. S. Ahmed, 'A Review on the Effect of Metal Oxide Nanoparticles on Tribological Properties of Biolubricants', 2023, *American Chemical Society*. doi: doi:10.1021/acsomega.3c08279.

[47] D. Napierska, L. C. J. Thomassen, D. Lison, J. A. Martens, and P. H. Hoet, 'The nanosilica hazard: another variable entity', *Particle and Fibre Toxicology 7 (2010) 39*, doi: doi:10.1186/1743-8977-7-39.

[48] B. Fubini, M. Ghiazza, and I. Fenoglio, 'Physico-chemical features of engineered nanoparticles relevant to their toxicity', *Nanotoxicology 4 (2010) 347–363*, doi: doi: 10.3109/17435390.2010.509519.

[49] K. Holmberg and A. Erdemir, 'Influence of tribology on global energy consumption, costs and emissions', Sep. 01, 2017, *Tsinghua University Press*. doi: 10.1007/s40544-017-0183-5.

[50] 'ASTM D4052-22; Standard Test Method for Density, Relative Density, and API Gravity of Liquids by Digital Density Meter. ASTM: West Conshohocken, PA, USA, 2022.' Accessed: Oct. 30, 2024. [Online]. Available: https://www.astm.org/d4052-22.html.

[51] 'ASTM D445-24; Standard Test Method for Kinematic Viscosity of Transparent and Opaque Liquids (and Calculation of Dynamic Viscosity). ASTM: West Conshohocken, PA, USA, 2024.' Accessed: Oct. 30, 2024. [Online]. Available: https://www.astm.org/d0445-24.html.

[52] 'ISO 2909:2002; Petroleum Products–Calculation of Viscosity Index from Kinematic Viscosity. International Organization for Standardization: Geneva, Switzerland, 2002.'.

[53] 'ASTM D4739-17; Standard Test Method for Base Number Determination by Potentiometric Hydrochloric Acid Titration. ASTM: West Conshohocken, PA, USA, 2017'. Accessed: Oct. 30, 2024. [Online]. Available: doi:10.1520/D4739-17.

[54] 'ASTM D664-18e2; Standard Test Method for Acid Number of Petroleum Products by Potentiometric Titration. ASTM: West Conshohocken, PA, USA, 2018.' Accessed: Oct. 30, 2024. [Online]. Available: https://www.astm.org/d0664-18e02.html.

[55] V. Cortes, K. Sanchez, R. Gonzalez, M. Alcoutlabi, and J. A. Ortega, 'The performance of SiO2 and TiO2 nanoparticles as lubricant additives in sunflower oil', *Lubricants*, vol. 8, no. 1, Jan. 2020, doi: 10.3390/lubricants8010010.

[56] Gulzar M, et al. Dispersion Stability and Tribological Characteristics of TiO2/SiO2 Nanocomposite-Enriched Biobased Lubricant. Tribol Trans Jul. 2017;60(4):670–80. https://doi.org/10.1080/10402004.2016.1202366.

[57] Benedetti V, Cascioli A, Pecchi M, Baratieri M. Fast screening of catalyst performances in hydrothermal processes for biofuel production using differential scanning calorimetry. Bioresour Technol 2024;405:Aug. https://doi.org/10.1016/j.biortech.2024.130934.

[58] Pecchi M, Cascioli A, Maag AR, Goldfarb JL, Baratieri M. Uncovering the transition between hydrothermal carbonization and liquefaction using differential scanning calorimetry. Fuel Process Technol 2022;235:Oct. https://doi.org/10.1016/j.fuproc.2022.107349.

[59] H. Jiang, X. Hou, K. D. Dearn, D. Su, and M. Kamal Ahmed Ali, 'Thermal stability enhancement mechanism of engine oil using hybrid MoS2/h-BN nano-additives with ionic liquid modification', *Advanced Powder Technology*, vol. 32, no. 12, pp. 4658–4669, Dec. 2021, doi: 10.1016/j.apt.2021.10.015.

[60] Rattana-Amron T, Chotsuwan C. PRACTICAL METHODS TO DETERMINE THE THERMAL STABILITY OF MOTOR OILS. Petroleum and Coal Pet Coal 2019.

[61] Jedrzejczyk MA, et al. Lignin-based Additives for improved Thermo-Oxidative Stability of Biolubricants. ACS Sustain Chem Eng Sep. 2021;9(37):12548–59. https://doi.org/10.1021/acssuschemeng.1c02799.

[62] R. N. Sarma and R. Vinu, 'Current Status and Future Prospects of Biolubricants: Properties and Applications', Apr. 01, 2022, *MDPI*. doi: 10.3390/lubricants10040070.
[63] H. Piri, M. Renzi, and M. Bietresato, 'Technical Implications of the Use of Biofuels in Agricultural and Industrial Compression-Ignition Engines with a Special Focus on the Interactions with (Bio)lubricants', Jan. 01, 2024, *Multidisciplinary Digital Publishing Institute (MDPI)*. doi: 10.3390/en17010129.
[64] Heikal EK, Elmelawy MS, Khalil SA, Elbasuny NM. Manufacturing of environment friendly biolubricants from vegetable oils. Egypt J Pet Mar. 2017;26(1):53–9. https://doi.org/10.1016/J.EJPE.2016.03.003.
[65] S. J. Hettiarachchi, 'Enhancing engine oil performance using nanoparticles and biolubricants as additives', 2022. [Online]. Available: http://orcid.org/0000-0002-0489-270X.
[66] Z. Wang *et al.*, 'Tribological Properties of Nano-Scale Al2O3 Particles with Different Shapes as Lubricating Oil Additives', *J Mar Sci Eng*, vol. 12, no. 7, Jul. 2024, doi: 10.3390/jmse12071069.
[67] Ali MKA, Xianjun H. Role of bis(2-ethylhexyl) phosphate and Al2O3/TiO2 hybrid nanomaterials in improving the dispersion stability of nanolubricants. Tribol Int 2021;155:Mar. https://doi.org/10.1016/j.triboint.2020.106767.
[68] M. Fasehullah, F. Wang, S. Jamil, and M. S. Bhutta, 'Influence of Emerging Semiconductive Nanoparticles on AC Dielectric Strength of Synthetic Ester Midel-7131 Insulating Oil', *Materials*, vol. 15, no. 13, Jul. 2022, doi: 10.3390/ma15134689.
[69] Nagarajan T, et al. Tribological, oxidation and thermal conductivity studies of microwave synthesised molybdenum disulfide (MoS2) nanoparticles as nano-additives in diesel based engine oil. Sci Rep 2022;12(1):Dec. https://doi.org/10.1038/s41598-022-16026-4.
[70] Nagarajan T, Sridewi N, Wong WP, Walvekar R, Khalid M. Enhanced tribological properties of diesel-based engine oil through synergistic MoS2-graphene nanohybrid additive. Sci Rep 2023;13(1):Dec. https://doi.org/10.1038/s41598-023-43260-1.
[71] Nagarajan T, Sridewi N, Wong WP, Walvekar R, Khanna V, Khalid M. Synergistic performance evaluation of MoS2–hBN hybrid nanoparticles as a tribological additive in diesel-based engine oil. Sci Rep 2023;13(1):Dec. https://doi.org/10.1038/s41598-023-39216-0.
[72] K. Markandan, T. Nagarajan, R. Walvekar, V. Chaudhary, and M. Khalid, 'Enhanced Tribological Behaviour of Hybrid MoS2@Ti3C2 MXene as an Effective Anti-Friction Additive in Gasoline Engine Oil', *Lubricants*, vol. 11, no. 2, Feb. 2023, doi: 10.3390/lubricants11020047.
[73] Hernaiz M, et al. Study of the effect of ZnO Functionalization on the Performance of a fully Formulated Engine Oil. Nanomaterials 2023;13(18):Sep. https://doi.org/10.3390/nano13182540.
[74] H. A. Zaharin *et al.*, 'Tribological, Oxidation and Thermal Analysis of Advanced Microwave–Hydrothermal Synthesised Ti3C2Tx MXene as Additives in Outboard Engine Oil', *Lubricants*, vol. 11, no. 6, Jun. 2023, doi: 10.3390/lubricants11060264.